Geotech Geol Eng (2019) 37:1079–1094
https://doi.org/10.1007/s10706-018-0665-x

TECHNICAL NOTE

# Correlation of Geo-Mechanics Parameters with Uniaxial Compressive Strength and P-Wave Velocity on Dolomitic Limestone Using a Statistical Method

**Lei Wen · Zhou quan Luo · Shi jiao Yang · Ya guang Qin · Wei Wang**

Received: 20 March 2018 / Accepted: 11 August 2018 / Published online: 17 August 2018


**Abstract** This paper estimates the correlation between the physical and mechanical characteristics of dolomitic limestone. Forty samples were measured and the results were used to derive the empirical equations for the relations between the uniaxial compressive strength (UCS), elastic modulus ($E$), P-wave velocity ($v_p$), Poisson's ratio ($\mu$), point load strength, and density ($\rho$). The correlation results for the intact dolomitic limestone samples showed high correlation between UCS and the other parameters, and between $v_p$ and the other parameters. Determination of physical and mechanical characteristics in situ or in the laboratory is always a costly process. In this paper, correlation relationships were proposed using $v_p$ and UCS to evaluate the other parameters where the results were in good agreement. To validate the empirical equations, a Student's $t$ test was conducted on the test data; the calculated $t$-test values were much higher than the tabulated values, indicating a generally good, linear relationship among the physical and mechanical properties of the intact dolomitic limestone. The results suggest that the $v_p$ and UCS values of dolomitic limestone samples can be used to estimate the $\rho$, $\mu$, and $E$ of the intact rock.

**Keywords** Regression analyses · Geo-mechanics properties · Correlation relationship · Student's $t$ test

L. Wen (✉) · Z. Luo · Y. Qin · W. Wang
School of Resources and Safety Engineering, Central South University, Changsha 410083, China
e-mail: 821149277@qq.com

Z. Luo
e-mail: 389803820@qq.com

Y. Qin
e-mail: 846616975@qq.com

W. Wang
e-mail: 305334943@qq.com

S. Yang
Nuclear Resource Engineering College, University of South China, Hengyang 421001, Hunan, China
e-mail: 649292197@qq.com

## 1 Introduction

The geo-mechanical properties of a rock mass are fundamental in mining and civil construction design. However, the natural discontinuities and inhomogeneity of any given rock mass can create internal and external uncertainties when measuring such properties (Ozcelik et al. 2012; Mikaeil et al. 2013; Azadan and Ahangari 2014). Moreover, determining the physical and mechanical properties of rocks from deep mines or from highly fractured rocks in a laboratory or in the field can be expensive and time-consuming. These difficulties may be overcome if reliable empirical relationships could be determined among at least the most critical properties needed in the design process. Statistical analysis and regression analysis were used in previous studies to derive the empirical correlation among various geo-mechanical properties of rocks. Sharma et al. (2011) examined the relationships between the Schmidt hammer rebound numbers and the impact strength index, slake durability index, and P-wave velocity using empirical equations. Diamantis et al. (2011) investigated the relationships between the P-wave velocity and the physical and mechanical properties and petrographic characteristics of peridotites from central Greece using simple regression analyses and confidence intervals. These empirical relationships were used to estimate the geo-mechanics properties of a rock mass.

Sonic and ultrasonic measurements are also useful tools for assessing rock properties and have been used in previous studies. Ultrasonic methods are nondestructive and relatively easy to use, both in the field and in the laboratory. Ultrasonic methods are being increasingly employed in mining, geological, and underground engineering to determine the dynamic properties of rocks for use in in situ and laboratory experiments. The P-wave velocity of a rock is closely related to the intact rock structure and mineral compositions. Zhou et al. (2014) examined a slope damaged by excavation at a hydropower station site using acoustic testing technology. Many investigators demonstrated that a rock's P-wave velocity is strongly correlated with its geo-mechanical properties. Some of these empirical relationships are listed in Table 1. In this study we investigate the correlation between the physical and mechanical properties of dolomitic limestone samples using P-wave velocities and uniaxial compressive strength tests.

## 2 Study Area and Samples

### 2.1 Study Area

The study site was the Huize lead and zinc mine, located between the Yunnan and Guizhou provinces in southwest China (Fig. 1). The landform in the study area is complex and includes alpine morphologies, gorges, and riverine landscapes. The Niu-Lan river flows through the mining area at an elevation of 1561 m. The peak elevation is 2668.9 m and the elevation of the mine entrance is 2538 m, a relative elevation difference of close to 1000 meters. Multiple faults run through the mining area, leading to the formation of cracks in the rock mass. In addition to the faults, the high stress in the deep parts (1500 m) of the rock mass (42.34–45.95 MPa, based on three tests) causes fragmentation of the rock mass. Therefore, it is very difficult to obtain intact cores from depths over 2000 m. Due to high in situ stress of the study site the drilled cores were fragmented and discs were cut from the cores (Fig. 2). The main aim of this study is to predict the physical and mechanical parameters of the rock in a deep mine using empirical relationships based on selected derived parameters. This can reduce test costs and save time when only a small number of samples can be obtained.

The geological structure of the study area (Fig. 3) includes the north-east to south-west fold and fault, forming an anticline. The Kuang-shan Chang fault, the Qi-lin Chang fault and the Yin-chang Po fault form three overlapping tile structures. The north–south Dong Tou fault also affects the study area. The sampling was carried out between the Qi-lin Chang fault and the Yin-chang Po fault, closer to the Qi-lin Chang fault. In this area, the upper strata of the Devonian system, the upper Paleozoic Carboniferous system, and the Permian strata are widely distributed. Mount E-mei basalt along the Qi-lin Chang reverse fault is exposed in the southern and western areas of the mining area, and there are a few weathering residues in the middl of the area.

### 2.2 Rock Samples

Forty samples were obtained from the mine at a depth of 1500 m below ground level. The rock samples were mainly dolomitic limestone and were fresh to slightly weathered. To preserve the in situ conditions, the rock specimens were saturated prior to measuring the rock properties. The specimens were classified as fine to medium dolomitic limestone of the carboniferous system in the Permian strata. An image of the dolomitic limestone taken in situ is shown in Fig. 4. Several macroscopic structures and visible features were observed in the rock mass. Signs of medium-grade dynamic metamorphism associated with tectonic and ore-forming fluid activities were found in the rock mass; this included evidence of pyritization (oxidized into limonite), development of silicide, chloritization, epidotization, and calcite and hydrothermal alteration. The most obvious indication of such metamorphism were calcite veins observed on

**Table 1** Empirical relation reported between rock mechanical parameters and P-wave velocity

| Researches | Empirical relation | $R^2$ |
|---|---|---|
| Tugrul and Zarif (1999) | $UCS = 35.54v_p - 55$ | 0.64 |
| Kahraman (2001) | $UCS = 9.95v_p^{1..21}$ | 0.69 |
| Yasar and Erdogan (2004) | $UCS = 31.5v_p - 63.7$ | 0.80 |
| Sousa et al. (2005) | $UCS = 22.032v_p^{1.247}$ | 0.72 |
| Sharma and Singh (2008) | $UCS = 64.2v_p - 117.99$ | 0.90 |
| Cobanoglu and Celik (2008) | $UCS = 56.71v_p - 192.93$ | 0.67 |
| Diamantis et al. (2009) | $UCS = 110v_p - 515.56$ | 0.81 |
| Khandelwal and Singh 2009 | $UCS = 133.3v_p - 227.17$ | 0.96 |
| Sharma and Singh (2008) | $UCS = 36v_p - 45.37$ | 0.93 |
| Diamantis et al. (2011) | $UCS = 0.14v_p - 889.33$ | 0.83 |
| Kurtulus et al. (2012) | $UCS = 0.0675v_p - 245.13$ | 0.92 |
| Sarkar et al. (2012) | $UCS = 0.038v_p - 50$ | 0.93 |
| Altindag (2012) | $UCS = 0.258v_p^{1.194}$ | 0.79 |
| Khandelwal (2013) | $UCS = 0.033v_p - 34.83$ | 0.87 |
| Abdolazim and Rassoul (2015) | $UCS = 0.026v_p - 20.47$ | 0.91 |
| Current study | $UCS = 0.034v_p - 86.36$ | 0.80 |
| Khandelwal and Singh (2009) | $E = 4.9718v_p - 7151$ | 0.97 |
| Kurtulus et al. (2012) | $E = 0.0015v_p - 2.516$ | 0.74 |
| Diamantis et al. (2011) | $E = 0.041v_p - 264.15$ | 0.81 |
| Altindag (2012) | $E = 0.919v_p^{1.9122}$ | 0.79 |
| Abdolazim and Rassoul (2015) | $E = 0.008v_p - 5.619$ | 0.89 |
| Current study | $E = 0.013v_p - 30.71$ | 0.83 |
| Kahraman and Yeken (2008) | $\rho = 0.213v_p - 1.256$ | 0.82 |
| Khandelwal and Singh (2009) | $\rho = 0.0011v_p - 0.0847$ | 0.97 |
| Diamantis, et al. (2011) | $\rho = 0.0027v_p - 12.02$ | 0.83 |
| Kurtulus et al. (2012) | $\rho = 0.0002v_p + 1.7752$ | 0.87 |
| Sarkar et al. (2012) | $\rho = 0.00028v_p + 1.59$ | 0.93 |
| Khandelwal (2013) | $\rho = 0.202v_p + 1.79$ | 0.86 |
| Abdolazim and Rassoul (2015) | $\rho = 0.0002v_p + 1.94$ | 0.89 |
| Current study | $\rho = 4.545 \times 10^{-5}v_p + 2.54$ | 0.67 |
| Khandelwal (2013) | $\mu = 8 \times 10^{-9}(v_p)^2 - 2 \times 10^{-5}v_p + 0.222$ | 0.849 |
| Current study | $\mu = 0.52 - \frac{91}{30.33+(v_p)^{0.69}}$ | 0.97 |

*UCS*—uniaxial compressive strength, $v_p$—P-wave velocity, *E*—elastic modulus, $\rho$—density, $\mu$—Poisson's ratio

the fresh surface of the rock mass, as seen in Fig. 4. The rock samples are light in color, composed mainly of gray and light gray, medium to thick lamellar to cryptic limestone, and Tiger porphyritic dolomitic limestone with thick layered dolomite. The samples are mainly limestone, with Tiger porphyry intercalated with dolomitic limestone. The rock contains large amounts of calcite and siliceous nodules or lenses, and a small amount of shale and breccia limestone. Dolomite veins, calcite and pyrite can be observed clearly in the joint planes of the rock mass, as shown in Fig. 4.

The rock testing was performed on cylindrical drill core samples of dimensions (length × diameter) 100 × 50 mm or 130 × 63 mm, as seen in Fig. 5. To reduce the influence of the sample size on the strength testing process, the diameters of the cylindrical rock specimens were prepared with a length-to-diameter ratio of 2.0–2.1. The two ends of each specimen were ground and lapped parallel, to an

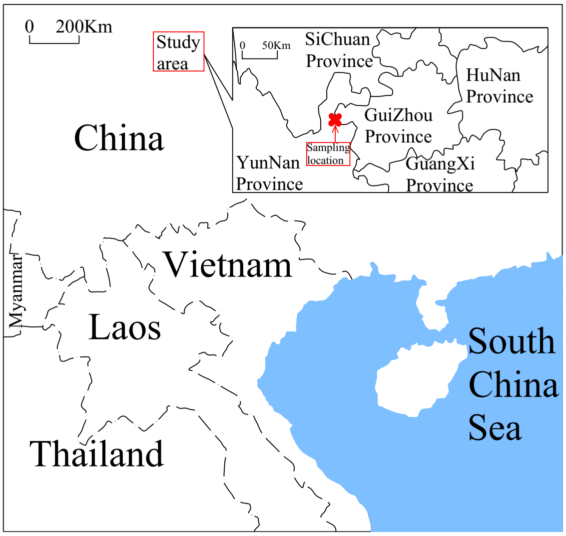


**Fig. 1** Maps showing the study area

accuracy of ± 0.3 mm. The core surfaces must be parallel to prevent surface irregularities; the surface roughness of the two ends of the specimen deviated by only ± 0.05 mm.

## 3 Determining the Physical and Mechanical Parameters

Of the physical and mechanical parameters of a rock, the uniaxial compressive strength (UCS) and P-wave velocity ($v_p$) are the two most representative parameters. To understand the characteristics of the rock and its behavior under various engineering conditions, a mechanical strength test of the rock must be performed first. The most important strength test is the uniaxial compressive strength test. The UCS of a rock is an important indicator of the rock's bearing capacity. The elastic modulus ($E$) and Poisson's ratio ($\mu$) of a rock sample can be derived from the results of the uniaxial compressive strength test (Eqs. 1 and 2). The P-wave velocity of an intact rock block mainly depends on $E$, $\mu$, and the density ($\rho$), as shown in Eq. (3). In addition, the microstructure and water inside the rock can also greatly influence the UCS and $v_p$. Thus, it is necessary to study the empirical relationship between $v_p$ and UCS and other parameters. Using reliable empirical relationships to evaluate the physical and mechanical parameters of rock samples can effectively reduce experimental costs and time. Thus, this study can have broad engineering applications.

$E$ is the elastic modulus, $\varepsilon_{radial}$ is the radial strain, $\varepsilon_{axial}$ is the ax

$$E = \frac{\text{UCS}}{\varepsilon_{axial}} \tag{1}$$

$$\mu = \left| -\frac{\varepsilon_{radial}}{\varepsilon_{axial}} \right| \tag{2}$$

$$v_p = \sqrt{\frac{E(1-\mu)}{\rho(1+\mu)(1-2\mu}} \tag{3}$$

where $E$ is elastic modulus, $\varepsilon_{radial}$ is radial strain, $\varepsilon_{axial}$ is axial strain, $\mu$ is Poisson's ratio and $\rho$ is density.

**Fig. 2** Discs from drilled cores obtained from 1500 m depth

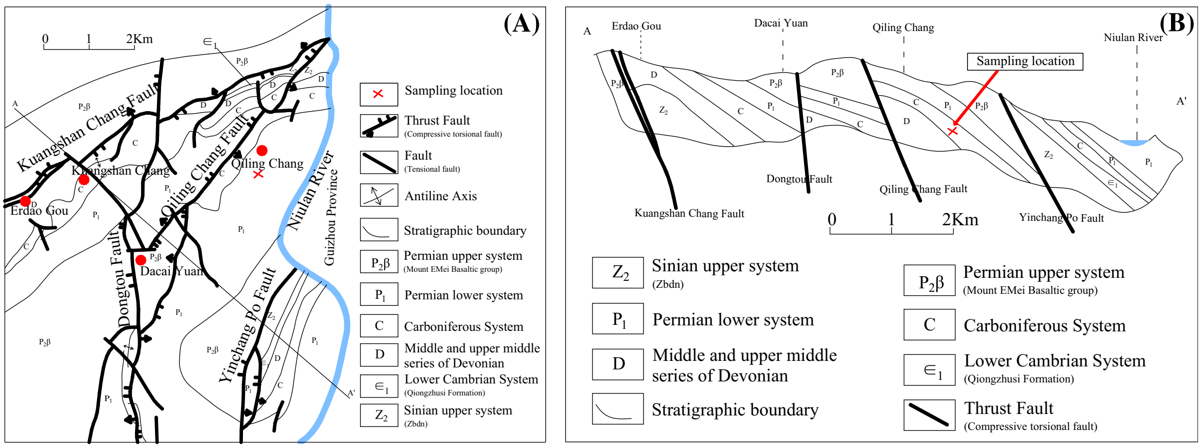


**Fig. 3** Geological structure; **a** plane map of the geological structure; **b** A–A' geologic sections

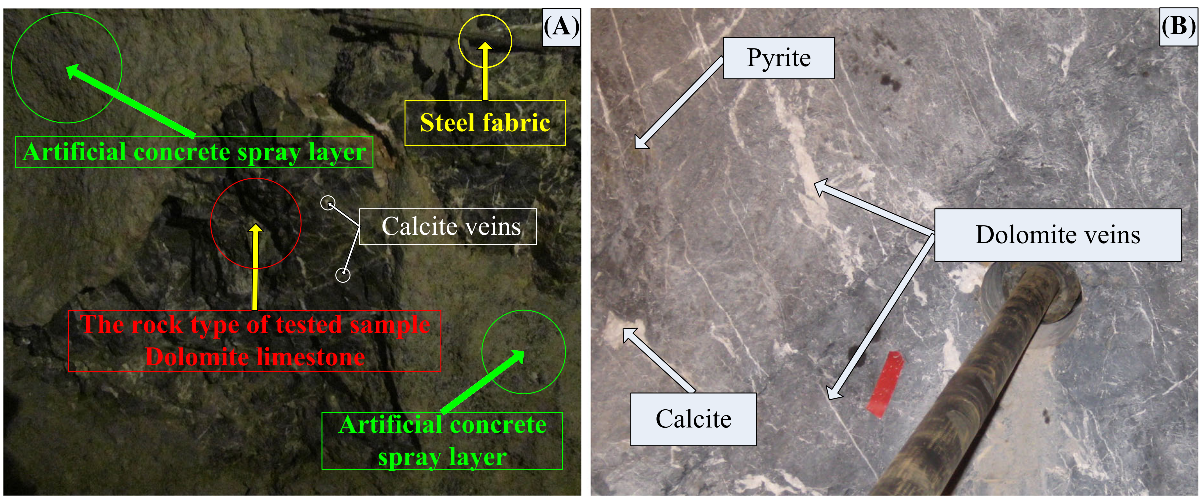


**Fig. 4** Photos of dolomite limestone taken in the study site; **a** supported area; **b** non-supported area

## 3.1 Testing Instruments and Procedures

Various standard tests were performed on the prepared samples to determine the properties of the rocks from the study area. The density and porosity were measured according to the International Society for Rock Mechanics (ISRM) standards (1981). The density of the dolomitic limestone was calculated as the ratio of the specimen mass divided by its volume. The $v_p$ value was determined using an acoustic emission testing system (ADLINK, USA) according to ISRM suggested testing methods (2007). The deformation was recorded by strain gauges attached to the prepared core samples. The elastic modulus was obtained from the gradient of the stress–strain curves using the tangent method. To eliminate the friction effect at the top and bottom ends of the sample, the top and bottom surfaces of the core specimens were ground and covered with petroleum jelly. The $v_p$ value was obtained as shown in Fig. 6a. To ensure the accuracy of the test results, three tests were carried out on each sample and the mean value of the three measurements was obtained. The uniaxial compressive strength was determined using a hydraulic servo mechanical testing machine (INSTRON-1346, INSTRON, Melbourne, Australia) following ASTM (1986) standards, as shown in Fig. 6.

**Fig. 5** Rock Samples taken from 1000 m depth; original samples (left) and prepared samples (right)

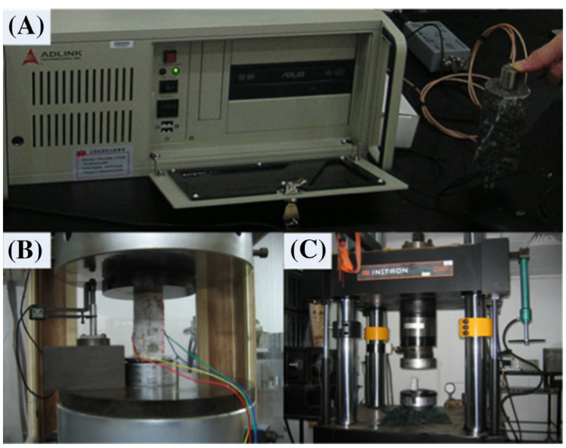


**Fig. 6** Testing setup; **a** the ADLINK acoustic emission testing system; **b**, **c** the hydraulic servo mechanical testing machine (INSTRON-1346))

### 3.2 Physical and Mechanical Parameters

The physical and mechanical parameters of the sedimentary rock samples determined by the laboratory tests are shown in Table 2. The values of $\rho$ and $\mu$ were found to be within a relatively limited range for the saturated samples, but the values of $E$, $v_p$, UCS and the point load index ($I_s$) extended over a broader range. $\rho$ was within 2.683–2.841 g/cm$^3$, with a mean value of 2.740 g/cm$^3$.

The $I_s$ values, measured on irregular blocks using a digital point load test system based on ISRM guidelines (1985), were within 0.84–6.09 MPa, with a mean value of 3.10 MPa. The $v_p$ values were measured according to the American Standard Testing Method (ASTM) standards (1983) for measuring the travel time of ultrasound pulses in a rock specimen. The $v_p$ values fluctuated between 3161 and 6148 m/s, with a mean value of 4293 m/s. The $E$ values varied considerably, from 6.405 to 47.936 GPa, with a mean value of 25.789 GPa. The UCS were within a very broad range (15.765–124.74 MPa), with a mean value of 60.07 MPa. The significant fluctuations of UCS, $v_p$, and $E$ can be attributed to the degree of weathering of the samples, their moisture content, and their inherent mineral compositions.

## 4 Regression Analyses

The physical and mechanical parameters of rocks are strongly related to UCS and $v_p$. Many researchers have also described the empirical relationship among them. However, the physical and mechanical properties of rocks are influenced by many factors such as the rock type, composition, porosity, joints, and water content. In this study, linear and nonlinear regression analyses were used to quantify the relationships among the

**Table 2** Geotechnical properties of studied samples

| No. | Elastic modulus $E$ (GPa) | P-wave velocity $v_p$ (m/s) | UCS (MPa) | Density $\rho$ (g/cm$^3$) | Poisson's ratio $\mu$ | $I_s$ (MPa) |
|---|---|---|---|---|---|---|
| 1 | 19.75 | 4259 | 41.99 | 2.738 | 0.25 | 2.67 |
| 2 | 42.875 | 5295 | 106.29 | 2.798 | 0.28 | 5.68 |
| 3 | 43.275 | 5312 | 110.13 | 2.828 | 0.28 | 5.72 |
| 4 | 33.025 | 5566 | 83.11 | 2.789 | 0.30 | 4.49 |
| 5 | 30.25 | 4644 | 74.75 | 2.789 | 0.27 | 4.43 |
| 6 | 37.575 | 4889 | 75.85 | 2.741 | 0.27 | 4.11 |
| 7 | 24.05 | 4181 | 45.64 | 2.72 | 0.25 | 2.83 |
| 8 | 26.7 | 4951 | 71.74 | 2.75 | 0.28 | 3.61 |
| 9 | 12.175 | 4097 | 44.86 | 2.71 | 0.25 | 2.28 |
| 10 | 27.64 | 4176 | 43.9 | 2.722 | 0.25 | 2.19 |
| 11 | 47.936 | 6016 | 113.2 | 2.789 | 0.30 | 5.74 |
| 12 | 7.588 | 3321 | 32.13 | 2.709 | 0.21 | 2.18 |
| 13 | 45.136 | 6148 | 124.74 | 2.841 | 0.32 | 6.09 |
| 14 | 26.584 | 4015 | 65.76 | 2.748 | 0.24 | 3.39 |
| 15 | 22.9 | 4049 | 35.38 | 2.717 | 0.24 | 1.83 |
| 16 | 22.375 | 3777 | 73.06 | 2.7654 | 0.23 | 3.71 |
| 17 | 13.5 | 3405 | 50.87 | 2.718 | 0.22 | 2.29 |
| 18 | 14.44 | 3759 | 36.29 | 2.699 | 0.23 | 2.13 |
| 19 | 6.6 | 3227 | 13.97 | 2.674 | 0.20 | 0.97 |
| 20 | 22.84 | 4186 | 71.81 | 2.799 | 0.25 | 3.58 |
| 21 | 35.074 | 5040 | 84.95 | 2.756 | 0.28 | 3.93 |
| 22 | 27.525 | 4327 | 41.686 | 2.7 | 0.26 | 2.18 |
| 23 | 27.508 | 4591 | 55.142 | 2.715 | 0.27 | 2.89 |
| 24 | 24.449 | 4375 | 63.465 | 2.736 | 0.26 | 3.12 |
| 25 | 44.063 | 5572 | 115.765 | 2.823 | 0.30 | 5.18 |
| 26 | 34.786 | 4417 | 77.695 | 2.778 | 0.26 | 3.56 |
| 27 | 43.865 | 5461 | 106.012 | 2.775 | 0.30 | 4.96 |
| 28 | 19.546 | 3389 | 38.069 | 2.726 | 0.21 | 1.89 |
| 29 | 25.647 | 3867 | 49.859 | 2.727 | 0.24 | 2.52 |
| 30 | 14.184 | 3521 | 40.337 | 2.7 | 0.22 | 2.36 |
| 31 | 16.822 | 3560 | 36.321 | 2.716 | 0.23 | 1.86 |
| 32 | 38.239 | 4529 | 69.152 | 2.756 | 0.26 | 3.21 |
| 33 | 21.391 | 4052 | 29.765 | 2.689 | 0.25 | 1.61 |
| 34 | 25.414 | 4076 | 71.751 | 2.742 | 0.25 | 3.58 |
| 35 | 36.434 | 4460 | 87.77 | 2.766 | 0.26 | 4.27 |
| 36 | 6.405 | 3214 | 15.765 | 2.674 | 0.20 | 0.84 |
| 37 | 15.797 | 3161 | 18.356 | 2.685 | 0.19 | 1.26 |
| 38 | 14.23 | 3565 | 17.26 | 2.692 | 0.23 | 1.47 |
| 39 | 12.361 | 3475 | 28.998 | 2.699 | 0.23 | 1.51 |
| 40 | 20.588 | 3819 | 39.294 | 2.683 | 0.24 | 1.94 |

Where, *UCS* represents the uniaxial compressive strength and $I_s$ is the point load strength

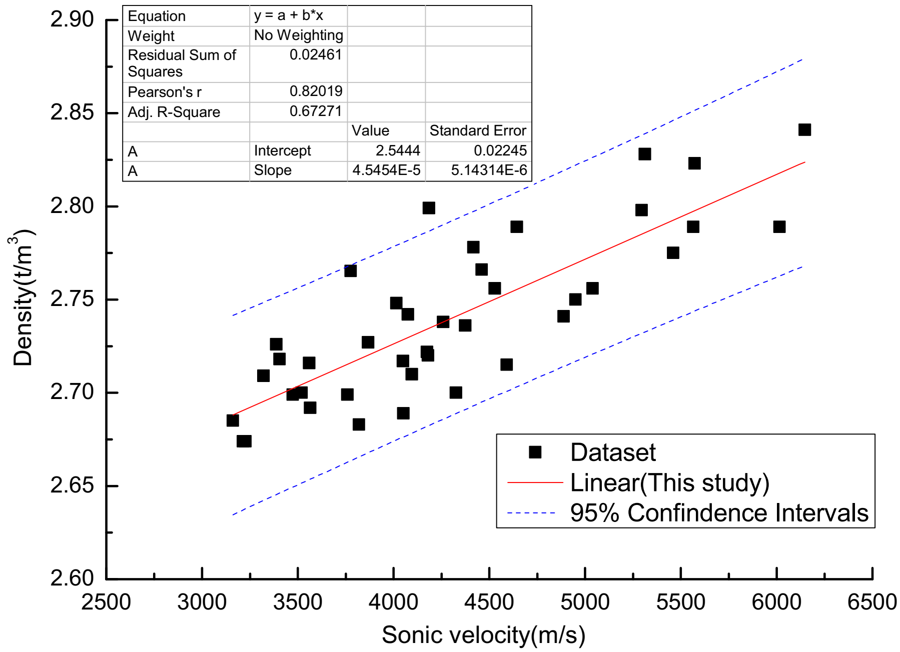


**Fig. 7** Variation of $\rho$ with increasing $v_p$

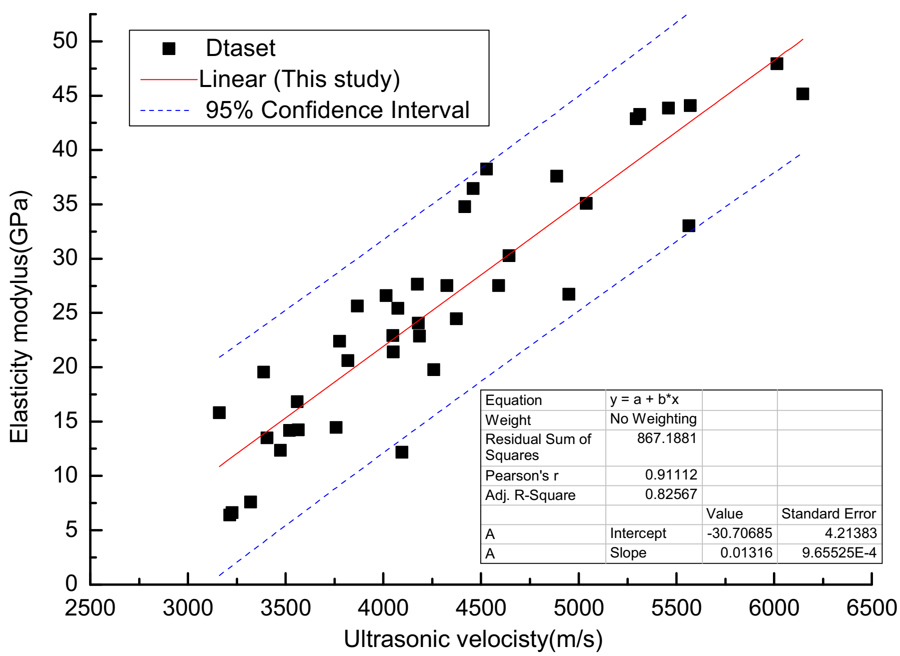


**Fig. 8** Variation of $E$ with increasing $v_p$

various physical and mechanical properties ($v_p$, $I_s$, UCS, $\rho$, $E$, and $\mu$) of the sedimentary rock samples. For convenience and practical testing considerations the empirical relations between $v_p$ and the physical and mechanical parameters UCS, $\rho$, $E$, and $\mu$ were derived, then the empirical relations between UCS and the physical and mechanical parameters $I_s$, $\rho$, $E$, and $\mu$ were determined. The confidence intervals were set at 95%, and the correlation coefficient $R^2$ for each regression was calculated when determining the equation of the line of best fit for each regression.

## 4.1 Relationships Between $v_p$ and the Other Rock Parameters

It is generally accepted that the mechanical properties of a rock sample increase linearly with increasing $v_p$ values. Our tests were designed to find the correlation between $v_p$ and $\rho$, $E$, $\mu$, and UCS. All the parameters showed a reasonable linear relationship with a high $R^2$ value, except for $\mu$, where a high coefficient of determination was obtained for the logistic function. The best-fit relationships are shown in Figs. 7, 8, 9 and 10 and are quantified in Eqs. (4)–(7).

$$\rho = 4.545 \times 10^{-5} v_p + 2.54 \quad R^2 = 0.67 \tag{4}$$

$$E = 0.013 v_p - 30.71 \quad R^2 = 0.83 \tag{5}$$

$$\mathrm{UCS} = 0.034 v_p - 86.36 \quad R^2 = 0.80 \tag{6}$$

$$\mu = 0.52 - \frac{91}{30.33 + (v_p)^{0.69}} \quad R^2 = 0.97 \tag{7}$$

where UCS is the uniaxial compressive strength, in MPa, determined from the unconfined compression test; $E$ is in GPa; $v_p$ is in m/s; $\rho$ is in g/cm$^3$; and $\mu$ is dimensionless. $R^2$ is the correlation ratio for the linear/nonlinear regression analysis results.

The relations between $v_p$ and $E$, UCS, and $\mu$ are best expressed by Eqs. (5), (6), and (7) ($R^2$ = 0.83, $R^2 = 0.8$, and $R^2 = 0.97$, respectively), compared with Eq. (4) ($R^2 = 0.67$) which expresses the best fit between $v_p$ and $\rho$. Many researchers found a close correlation between $v_p$ and the geo-mechanical properties; however, these empirical equations are related to specific rocks of certain origins and may not apply to other rock types.

As shown above, Eqs. (1)–(3) indicate that $\rho$, $E$ and UCS have a good positive linear relation with $v_p$, although the $R^2$ value in Eq. (1) is relatively low. Equation (4) shows that $\mu$ has a good positive nonlinear relation with $v_p$. These results indicate that $\rho$, $E$, $\mu$ and UCS increase with increasing $v_p$. However, these empirical relations need to be validated by the Student's $t$ test (see Sect. 5).

## 4.2 Relationships Between the UCS Value and the Other Rock Parameters

Previous research (Gunsallus and Kulhawy 1984; Panek and Fannon 1992; Singh and Singh 1993; Kahraman 2001) provided empirical relations between UCS and $I_s$. Similar to Sect. 4.1, we determined the

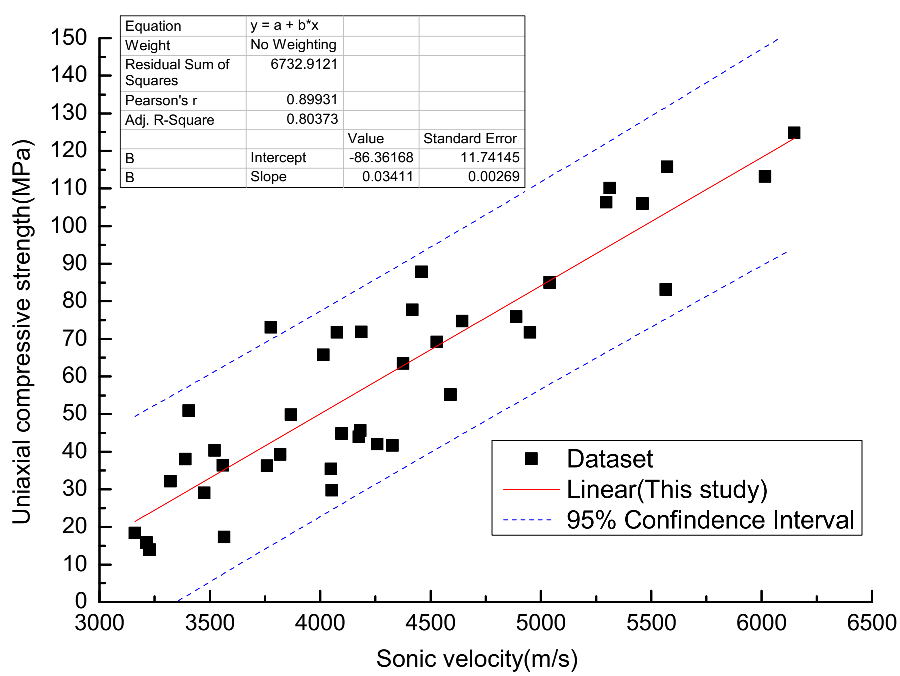


**Fig. 9** Variation of UCS with increasing $v_p$

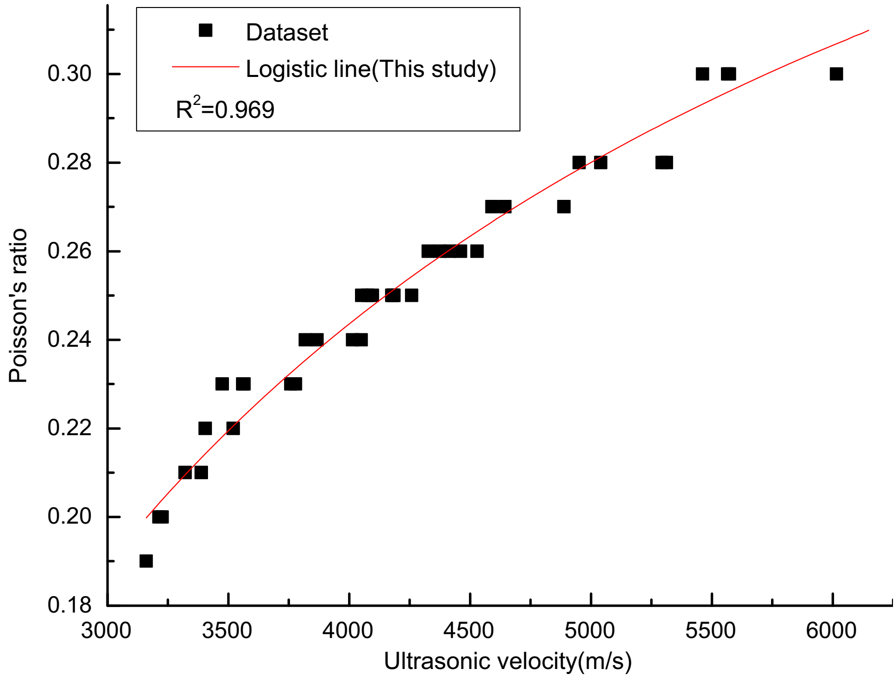


**Fig. 10** Variation of $\mu$ with increasing $v_p$

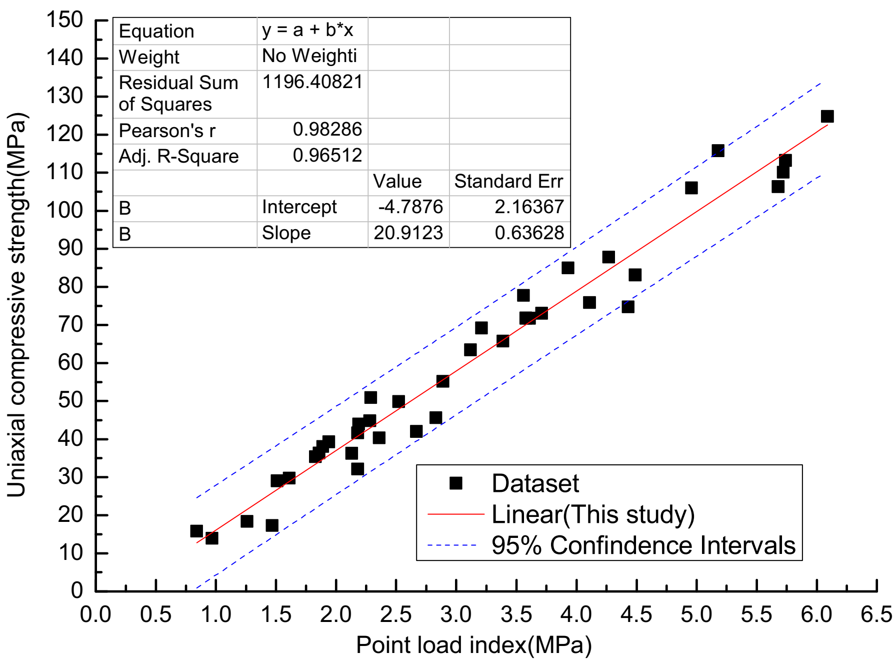


**Fig. 11** Variation of UCS with increasing $I_s$

relationships between UCS, the most fundamental rock strength parameter, and the rock's other physical and mechanical properties (Figs. 11, 12, 13 and 14). The regression lines for $E$, $\rho$, and $\mu$ estimated from the UCS value using the empirical equations derived in this research can be expressed as

$$\rho = 0.0013 \times \text{UCS} + 2.657 \quad R^2 = 0.871 \tag{8}$$

$$E = 0.347 \times \text{UCS} + 4.95 \quad R^2 = 0.825 \tag{9}$$

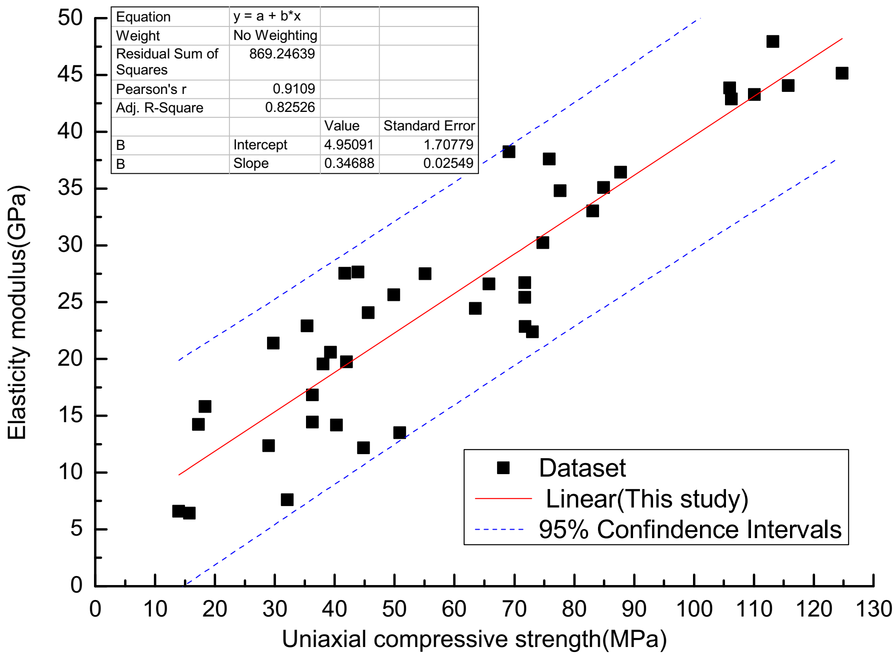


**Fig. 12** Variation of *E* with increasing UCS

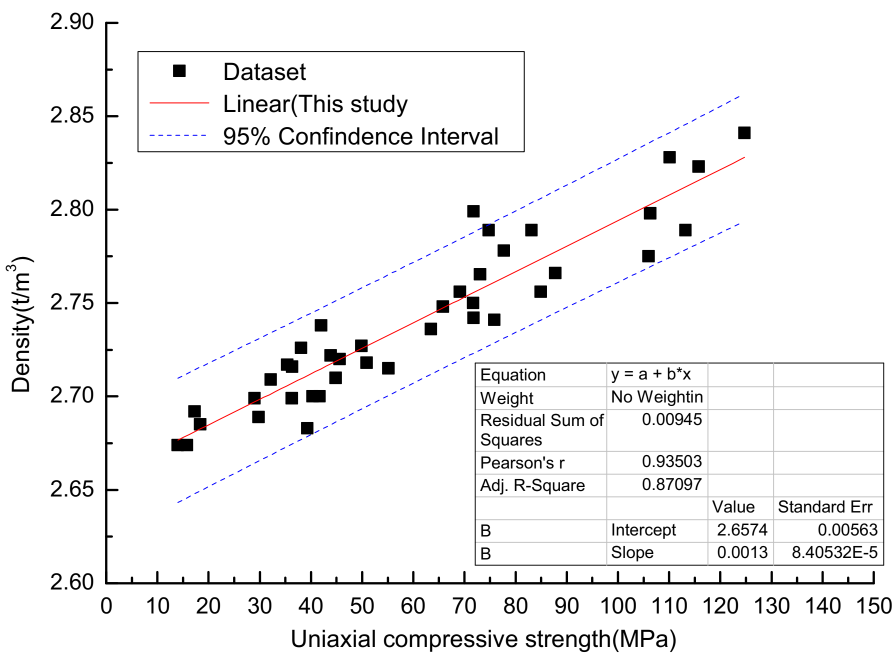


**Fig. 13** Variation of $\rho$ with increasing UCS

$$\mu = 8.767 \times 10^{-4} \times \text{UCS} + 0.199 \quad R^2 = 0.743 \qquad (10)$$

$$\text{UCS} = 20.91 \times I_s - 4.79 \quad R^2 = 0.956 \qquad (11)$$

where $I_s$ represents the point load index, in MPa.

Figures 11, 12, 13 and 14 show the best results of the linear regression analyses, where all the raw data are within the confidence intervals. The physical and mechanical parameters ($E$, $\rho$, $I_s$ and $\mu$) increase linearly with increasing UCS. In these estimates, the determination coefficients ($R^2$) of all the formulas (Eqs. 8–11) are very good. The highest determination coefficient was found for Eq. (11), suggesting that

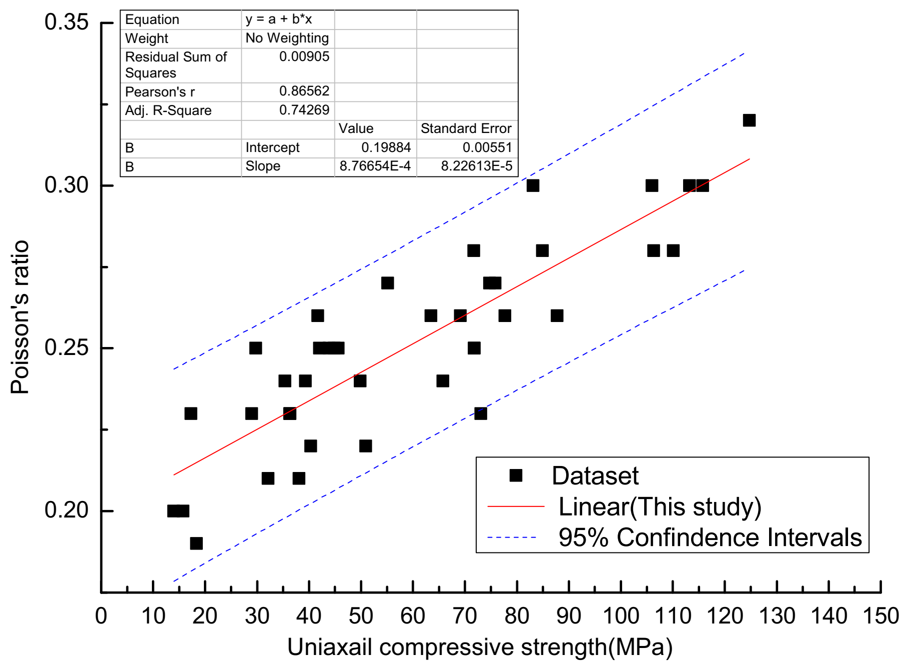


**Fig. 14** Variation of $\mu$ with increasing UCS

UCS can be predicted accurately using $I_s$ and Eq. (11). The coefficients $\rho$, $E$, and $\mu$ from Eqs. (8), (9), and (10), respectively, were also determined with reasonable accuracy, suggesting that properties such as $\rho$, $E$, and $\mu$ are closely related to the UCS value. Before applying these empirical relationships, their validity must be checked by the Student's $t$ test, as presented in Sect. 5.

The 1:1 slope line is used to evaluate the fit between the measured value and predicted value. The fitting line and 1:1 slope line are shown in Figs. 15 and 16 where the dataset located on the 1:1 slope line indicates an exact correlation. The larger the deviation from the slope line, the lower the accuracy. The $R^2$ values in Figs. 15 and 16 provide a good index for validating the reliability of the empirical relationship, indicating that $v_p$ and UCS can be used reliably to predict the other parameters.

## 5 Student's *t* Test

The high correlation between the rock mechanical parameters can be verified by the Student's $t$ test, assuming that the observations are chosen randomly and are normally distributed. Our test results were compared with the computed $t$ value and the tabulated $t$ value using the null hypothesis. The $t$-test compares the difference between two averages for the variation in the data. In Eq. (12), the numerator represents the absolute value of the difference between the two averages, and the denominator represents data dispersion. The expression for the $t$-test is given by:

$$t = \frac{|\overline{x_1} - \overline{x_2}|}{\sqrt{\frac{s_1^2}{n_1} + \frac{s_2^2}{n_2}}} \tag{12}$$

where $\overline{x_1}$ represents the tabulated mean, $\overline{x_2}$ represents the computed mean, $s_1^2$ represents the tabulated variance, $s_2^2$ represents the computed variance, and $n$ represents the number of samples.

Once the $t$ value is calculated, it is compared with the tabulated value. If the calculated value is higher than the tabulated one, this indicates good correlation. In Sect. 4, the confidence interval was set at 95% and the significance level was 0.05, obtaining a critical $t$ value of 1.684. The tabulated and calculated values are listed in Table 3. The calculated values of the $t$-test outperform the tabulated values, indicating that all the parameters have strong correlation among themselves.

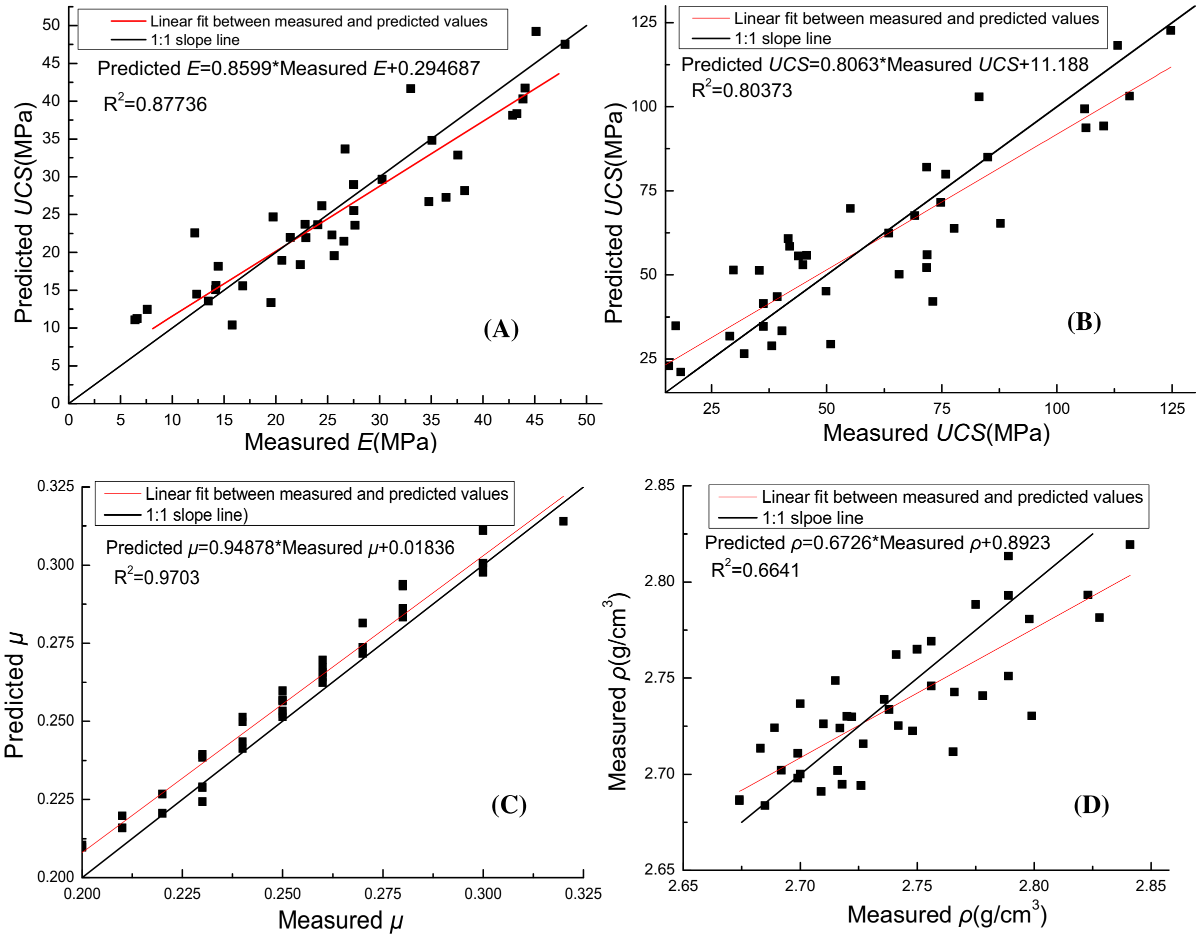


**Fig. 15** Cross-correlation of measured and predicted values from $v_p$

Thus, our results can be used to predict these parameters using the UCS value and the $v_p$ value.

## 6 Conclusions

In this paper, the physical and mechanical properties ($E$, UCS, $v_p$, $\mu$, and $\rho$) of dolomitic limestone were tested on 40 specimens. The results indicate significant correlations between the parameters $E$, $\mu$, and $\rho$ and the parameters $v_p$ and UCS. These empirical relations were expressed as equations which can be used to obtain important index properties of the dolomitic limestone and are accurate for general applications. The Student's $t$ test results showed higher values than the tabulated values, confirming that the physical and mechanical properties ($\rho$, $\mu$, and $E$) of dolomitic limestone in the Huize lead and zinc mine can be predicted using the proposed correlation equations. These equations may also apply to dolomitic limestone in other locations. Thus, the results of evaluating the physical and mechanical parameters of rocks presented in this paper may have broad applications in underground geotechnical engineering. Hence, in future research this method should be further investigated and applied to different rock types.

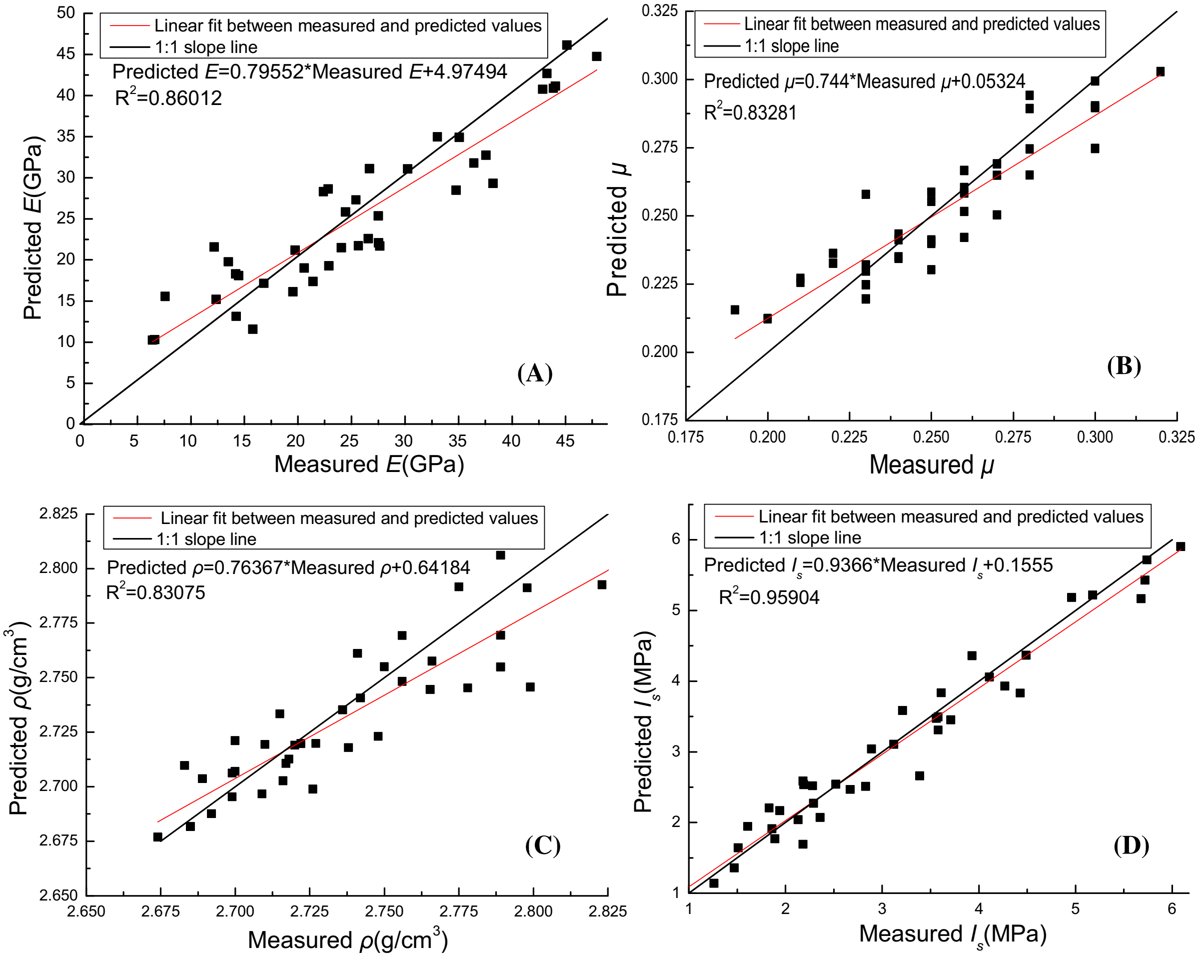


**Fig. 16** Cross-correlation of measured and predicted values from UCS

**Table 3** Tabulated and calculated *t* values of the Student's *t* test

| Rock tests | Student's *t* test | |
|---|---|---|
| | Calculated value | Tabulated value |
| Uniaxial compressive strength and P-wave velocity | 28.38 | 1.684 |
| Density and P-wave velocity | 28.78 | 1.684 |
| Poisson's ratio and P-wave velocity | 28.79 | 1.684 |
| Elasticity modulus and P-wave velocity | 28.62 | 1.684 |
| Point load index and uniaxial compressive strength | 12.12 | 1.684 |
| Density and uniaxial compressive strength | 12.20 | 1.684 |
| Poisson's ratio and uniaxial compressive strength | 12.73 | 1.684 |
| Elasticity modulus and uniaxial compressive strength | 6.86 | 1.684 |
| Poisson's ratio and elasticity modulus | 14.19 | 1.684 |
| Poisson's ratio and density | 37.16 | 1.684 |
| Elasticity modulus and density | 12.81 | 1.684 |

**Acknowledgements** The authors would like to express their deepest gratitude to the reviewers and the editors for their comments and suggestions, which helped improve the manuscript. This research was supported by the National Key R&D Program of China during the Thirteenth Five-year Plan Period: The Continuous Mining Theory and Technology on Spatiotemporal Synergism of Multi-mining Areas within a Large Ore Block for Deep Metal Deposit (2017YFC0602901). The work detailed in this paper was also supported by the Graduate Students Exploring Innovative Projects Independent Program (2017zzts188).

## References

Abdolazim A, Rassoul A (2015) Empirical correlation of physical and mechanical properties of marly rocks with P wave velocity. Arab J Geosci 8:2069–2079. https://doi.org/10.1007/s12517-013-1235-4

Altindag R (2012) Correlation between P-wave velocity and some mechanical properties for sedimentary rocks. J South Afr Inst Min Metall 11(3):229–237

ASTM (1983) Test methods for ultra violet velocities determination. American Society for Testing and Materials, D 2845

ASTM (1986) Standard test method of unconfined compressive strength of intact rock core specimens. D 2938

Azadan P, Ahangari K (2014) Evaluation of the new dynamic needle penetrometer in estimating uniaxial compressive strength of weak rocks. Arab J Geosci 7(8):1–12. https://doi.org/10.1007/s12517-013-0921-6

Cobanoglu İ, Celik SB (2008) Estimation of uniaxial compressive strength from point load strength, Schmidt hardness and P-wave velocity. Bull Eng Geol Env 67(4):491–498. https://doi.org/10.1007/s10064-008-0158-x

Diamantis K, Gartzos E, Migiros G (2009) Study on uniaxial compressive strength point load strength index, dynamic and physical properties of serpentinites fromCentral Greece: test results and empirical relations. Eng Geol 108(3–4):199–207. https://doi.org/10.1016/j.enggeo.2009.07.002

Diamantis K, Bellas S, Migiros G, Gartzos E (2011) Correlating wave velocities with physical, mechanical properties and petrographic characteristics of peridotites from the Central Greece. Geotech Geol Eng 29(6):1049–1062. https://doi.org/10.1007/s10706-011-9436-7

Gunsallus KL, Kulhawy FH (1984) A comparative evaluation of rock strength measures. Int J Rock Mech Min Sci Geomech Abstr 21(5):233–248. https://doi.org/10.1016/0148-9062(84)92680-9

ISRM (1981) Rock characterization, testing and monitoring. ISRM suggested methods. Oxford, Pergamon, p 211

ISRM (1985) Suggested methods for determining point load strength. Int J Rock Mech Min Sci Geomech Abstr 22:51–60

ISRM (2007) The complete ISRM suggested methods for rock characterization, testing and monitoring, 1974–2006. In: Ulusay R, Hudson JA (eds) Suggested methods prepared by the commission on testing methods, International society for rock mechanics, Compilation Arranged by the ISRM Turkish National Group, Ankara, p 293

Kahraman S (2001) Evaluation of simple methods for assessing the uniaxial compressive strength of rock. Int J Rock Mech Min Sci 38(7):981–994. https://doi.org/10.1016/S1365-1609(01)00039-9

Kahraman S, Yeken T (2008) Determination of physical properties of carbonate rocks from P-wave velocity. Bull Eng Geol Env 67(2):277–281. https://doi.org/10.1007/s10064-008-0139-0

Khandelwal M (2013) Correlating P-wave velocity with the physico-mechanical properties of different rocks. Pure Appl Geophys 170(4):507–514. https://doi.org/10.1007/s00024-012-0556-7

Khandelwal M, Singh TN (2009) Correlating static properties of coal measures rocks with p-wave velocity. Int J Coal Geol 79(1–2):55–60. https://doi.org/10.1016/j.coal.2009.01.004

Kurtulus C, Bozkurt A, Endes H (2012) Physical and mechanical properties of serpentinized ultrabasic rocks in NW Turkey. Pure Appl Geophys 169(7):1205–1215. https://doi.org/10.1007/s00024-011-0394-z

Mikaeil R, Ataei M, Yousefi R (2013) Correlation of production rate of ornamental stone with rock brittleness indexes. Arab J Geosci 6(1):115–121. https://doi.org/10.1007/s12517-011-0311-x

Ozcelik Y, Bayram F, Yasitli NE (2012) Prediction of engineering properties of rocks from microscopic data. Arab J Geosci 6(10):3651–3668. https://doi.org/10.1007/s12517-012-0625-3

Panek LA, Fannon TA (1992) Size and shape effects in point load tests of irregular rock fragments. Rock Mech Rock Eng 25(2):109–140. https://doi.org/10.1007/BF01040515

Sarkar K, Vishal V, Singh TN (2012) An empirical correlation of index geo-mechanical parameters with the compressional wave velocity. Geotech Geol Eng 30(2):469–479. https://doi.org/10.1007/s10706-011-9481-2

Sharma PK, Singh TN (2008) A correlation between P-wave velocity, impact strength index, slake durability index and uniaxial compressive strength. Bull Eng Geol Env 67(1):17–22. https://doi.org/10.1007/s10064-007-0109-y

Sharma PK, Khandelwal M, Singh TN (2011) A correlation between Schmidt hammer rebound numbers with impact strength index, slake durability index and P-wave velocity. Int J Earth Sci 100(1):189–195. https://doi.org/10.1007/s00531-009-0506-5

Singh VK, Singh DP (1993) Correlation between point load index and compressive strength for quartzite rocks. Geotech Geol Eng 11(4):269–272. https://doi.org/10.1007/BF00466369

Sousa LMO, Río LMSD, Calleja L et al (2005) Influence of microfractures and porosity on the physico-mechanical properties and weathering of ornamental granites. Eng Geol 77(1):153–168. https://doi.org/10.1016/j.enggeo.2004.10.001

Tuğrul A, Zarif IH (1999) Correlation of mineralogical and textural characteristics with engineering properties of selected granitic rocks from Turkey. Eng Geol 51(4):303–317. https://doi.org/10.1016/S0013-7952(98)00071-4

Yasar E, Erdogan Y (2004) Correlating sound velocity with the density, compressive strength and Young's modulus of

carbonate rocks. Int J Rock Mech Min Sci 41(5):871–875. https://doi.org/10.1016/j.ijrmms.2004.01.012
Zhou JW, Yang XG, Xing HG et al (2014) Assessment of the excavation-damaged zone in a tall rock slope using acoustic testing method. Geotech Geol Eng 32(4):1149–1158. https://doi.org/10.1007/s10706-014-9767-2